Review History for "Micromechanical Influence of Fabric Anisotropy and Stress Path Dependency on Liquefaction Susceptibility in Granular Soil"

Mohammad Salimi, Nazanin Irani, Merita Tafili & Torsten Wichtmann 2025

Summary

The paper was sent to three reviewers. Dr. Mehdi Pouragha (Reviewer A) and Dr. Alejandro Martinez (Reviewer C) accepted the review. The reviewer B declined the review due to a lack of time. The reviewers remained anonymous during the entire review process and the authors were anonymous for the reviewers. After the reviewing process was complete, both reviewers agreed to disclose their identity. In Review Round 1, the reviewers provided a series of comments for the authors and required a revision of the manuscript. In Review Round 2, the reviewers recommended the manuscript for publication. Additionally, the reviewer A asked for a clarification of one issue.

Review Round 1

Author response (general)

The authors wish to thank the reviewers and editor for their time and efforts in reviewing our manuscript. We hope the modified manuscript is suitable for publication in the Journal of Open Geomechanics. In the following, detailed answers to the reviewer's comments are provided. Changes addressing the reviewers' remarks are highlighted in yellow in the 'Tracked Changes' version of the manuscript.

Reviewer A (Mehdi Pouragha)

The manuscript describes DEMxCFD simulations with elongated particle shapes subjected to undrained cyclic loading along different Lode angles until liquefaction is reached. Samples with different initial fabrics were prepared and their response at microscopic and macroscopic scales were examined. Multiple observations were made about the trends of secant shear modulus, pore pressure development, deviatoric strain, contact fabric, and coordination number.

The multiple combinations of the initial and loading conditions has led to an extensive and valuable dataset which was described and analysed to gain insights into the relation between the microscopic parameters, such as fabric and coordination number, and the macroscopic responses.

The manuscript is clearly written, well structured, and interesting to read. However, the reader cannot help but feel that the analyses offered remain too descriptive of the data, and does not delve deep enough to provide insight beyond what has previously been discussed in the literature.

The discussion in the Introduction jumps too quickly on to the current research, and inevitably misses a major part of the previous relevant studies on the change of fabric during cyclic and monotonic loadings, and its effect of global response. The list of the overlooked studies is too long. A few examples are below. I invite the authors to review the available literature more carefully and assess the novelty of their findings in comparison to the current state of knowledge.

- https://doi.org/10.1007/s11440-020-00942-8
- https://doi.org/10.1002/nag.3658
- https://doi.org/10.1007/s10035-019-0892-8
- https://doi.org/10.1002/nag.1091
- https://doi.org/10.1007/s10035-024-01397-4
- https://doi.org/10.1016/j.compgeo.2022.104800
- https://doi.org/10.1016/j.soildyn.2023.108343

Other more specific comments:

- On page 11, we read "Under monotonic loading, [..] the discrepancy between the loading direction and the direction of the contact-normal-based fabric tensor gradually diminishes [..]. This conclusion is evident in the results presented in Figures 13, where increasing the Lode angle does not significantly affect the final values of the fabric components at the end of the shearing." This argument is, at best, confusing, as it relates direction of fabric in the Euclidean space to the Lode angle which is not Euclidean and is a measure of third invariant of stress.
- Following Equation 6, it is said that the fabric describes the "spatial distribution" of contacts. The authors mean "directional distribution". Spatial distribution is related to homogeneity/inhomogeneity while directional distribution is related to isotropy/anisotropy.
- On Eq 8, the authors need to clarify how rattlers are handled, specifically since a connection is made between coordination number and the transition between slid-like and liquid-like response. Incidentally, the threshold of CN=4 that has been mentioned on page 12 is not a correct assessment and there is a rich thread of studies on this threshold (beyond refs [7] and [9]). The authors are enticed to check the literature in physics community on the effect of parameters such as pressure and friction on jamming transition and the associated coordination number, e.g. https://doi.org/10.1039/C9SM01932D
- The damping ratio of 0.7 used in this study is too high and may have a non-negligible effect on CN at the phase transition.
- On page 6, the discussion resorts to the concept of force chains to interpret the stiffness of different samples. The relation between the details of the force chains and the stiffness is not immediately clear to me since, for a given contact, the stiffness remains fixed irrespective of the intensity of the contact force. At any rate, such discussions require visualizing the force chain.
- In Equation 9 a double log formula is suggested to empirically fit the data. Such compounding exponents introduce excessive sensitivities are generally avoided. Incidentally, correlating parameters with total deviatoric strain is fundamentally problematic as the latter is reference-dependent and therefore, the correlations are often not generalizable.
- The manuscript attempts to correlate the different behaviour of the samples with the differences in their initial anisotropy. However, this anisotropy is clearly evolving (as is discussed towards the end of the manuscript). Therefore, it makes more sense to correlate the response at any given time to the current anisotropy. This becomes more meaningful to distinguish between the initial stages of tests, where the effect of the initial anisotropy is more obvious, with the later stages of the test where the contact anisotropy is becoming more aligned with stress.
- I cannot grasp the importance of the polynomial fits in Fig 8.

Reviewer C (Alejandro Martinez)

This paper presents a DEM-CFD study focused on the cyclic behavior of granular assemblies with a focus on the effects of fabric and stress anisotropies. The methods used are robust, the results are interesting, and they make a strong contribution to the literature. Before recommending for publication, there are a number of comments that I would like to share with the authors:

- One suggestion regarding the title is to add terms that relate to the fabric anisotropy since apart from the stress anisotropy this is the major focus of the paper.
- Sentence on the bottom left column of page 2 saying "This approach might be time-consuming and may not account for excess pore water pressure resulting from volume strain" – could you provide additional information regarding what this sentence specifically refer to?
- Regarding the same section as the previous comment, can you add more information regarding the benefits of using CFD coupling in DEM simulations over using the constant volume approximation?
- Last sentence of section 1: what does "its" refer to specifically in this sentence?
- Could you explain the reason for using the coordination number instead of the mechanical coordination number or particle connectivity, particularly since studies have shown that the latter parameters are more strongly correlated with the material's mechanical response?
- Could additional discussion be provided regarding what material is the simulated granular assembly intending to represent with regards to its particle shape, size, and gradation? For example, is the behavior intended to reproduce that of a specific clean sand?
- Related to the point above, it would be beneficial to include some data showing the ability of the DEM-CFM model to reproduce typical behaviors of granular materials, like stress dependency, stress dilatancy, and critical states. This could be addressed by including a section on parameter calibration.
- Could a reference be provided to put the void ratio value in context? For example, a state parameter or relative density would provide such context.
- Regarding the selection of the linear contact model, could the authors add some context related to the ability of this model to reproduce granular material behavior considering that the effective stress in the simulations is changing from the initial value of 100 kPa to close to zero in a liquefied state? This would cause a change in the stiffness in contacts in real granular materials, which is not considered by the linear contact model.
- A damping ratio of 0.7 is higher than typically used in DEM simulation. Could the authors provide information regarding the need to use of such a high value?
- Please include information regarding the criterion used to finish a given simulation. Is a given number of cycles applied, or is there a target ru or deviatoric strain?
- Please describe how the deviatoric strain is calculated.
- Please include the shearing rate used in the simulation and quantification of inertial numbers to indicate whether the tests are performed in quasi-static conditions.
- Please provide a more detailed description of the way in which the samples are sheared. For instance, what amplitude of deviator stress is applied to the samples? How do the individual stresses change during a simulation? Why are the deviatoric strains always positive? I would have expected them to be negative on the extension side. This could be addressed by including a figure showing how the three stress and strain components vary during an entire simulation. This point caused confusion for me as I read the paper.
- Please define the stress ratio.
- Regarding the sentence on page 6 saying "This phenomenon can be attributed to the orientation of force chains relative to particle geometry. In TR90 samples, force chains predominantly traverse the long axes of particles, whereas in TR0 samples, they pass through the shorter dimensions. Consequently, TR90 samples exhibit a more pronounced stiff behavior, necessitating a greater number of loading cycles to induce liquefaction" – this sentence describes the resulting observation. Could the authors provide discussion regarding the cause for this? i.e., why does having the force chains transversing the particle long axes results in additional stability?

- Regarding the sentence on page 6 saying “A reduction in Gsec can lead to greater strain accumulation, which may, in turn, cause increased pore water pressure due to the constant volume constraint” – I’m curious about the cause and effect relationship. The sentence indicates that a reduction in Gsec leads to pore water pressure. Couldn’t the relationship be the opposite? i.e. as pore pressures increase the Gsec decreases as a result of decreasing effective stress. Additional discussion would be appreciated.
- Regarding the sentence on page 6 saying “It is also evident that samples with bedding planes parallel to the major principal applied stress exhibit higher stiffness under identical strain levels and loading conditions” – it is not possible to see the higher stiffness because the results are provided in normalized form, which highlight the rate of degradation but not the relative stiffness magnitudes. Could the results also be presented in absolute form?
- First line on right column of page 9 – should it say an angle of 0 degrees of TR0 and TR90?
- Regarding Section 5.1 – are the trends in fabric evolution the same of TR45 and TR90 samples? Since the results of these are not presented, the insights of this section are limited to the effect of stress anisotropy.
- Could the prediction included in Fig. 10 be included in Fig. 6 to show the quality of the fit?
- Sentence on page 10 saying “For instance, Figures 13(a) and (b) show a decrease in Fx and Fy beyond a deviatoric strain level of q=3.4
- Can you please provide further discussion on the sentence on page 12 saying “These observations align with the results shown in Figures 3(a), (b), and (c), where the maximum stress ratio for TR0 samples is attained at a lower "q compared to TR45 and TR90 samples”?
- Is the CN = 4 limit applicable to all granular materials, or would it depend on gradation and particle shape?

Author response

REVIEWER A – 1. The manuscript describes DEMxCFD simulations with elongated particle shapes subjected to undrained cyclic loading along different Lode angles until liquefaction is reached. Samples with different initial fabrics were prepared and their response at microscopic and macroscopic scales were examined. Multiple observations were made about the trends of secant shear modulus, pore pressure development, deviatoric strain, contact fabric, and coordination number. The multiple combinations of the initial and loading conditions has led to an extensive and valuable dataset which was described and analysed to gain insights into the relation between the microscopic parameters, such as fabric and coordination number, and the macroscopic responses. The manuscript is clearly written, well structured, and interesting to read. However, the reader cannot help but feel that the analyses offered remain too descriptive of the data, and does not delve deep enough to provide insight beyond what has previously been discussed in the literature. The discussion in the Introduction jumps too quickly on to the current research, and inevitably misses a major part of the previous relevant studies on the change of fabric during cyclic and monotonic loadings, and its effect of global response. The list of the overlooked studies is too long. A few examples are below. I invite the authors to review the available literature more carefully and assess the novelty of their findings in comparison to the current state of knowledge.
• https://doi.org/10.1007/s11440-020-00942-8
• https://doi.org/10.1002/nag.3658
• https://doi.org/10.1007/s10035-019-0892-8
• https://doi.org/10.1002/nag.1091
• https://doi.org/10.1007/s10035-024-01397-4
• https://doi.org/10.1016/j.compgeo.2022.104800
• https://doi.org/10.1016/j.soildyn.2023.108343

Response:
We deeply appreciate the reviewer’s efforts to thoroughly review the paper and provide his/her insightful comments, which significantly contribute to the improvement of our manuscript. We have revised the introduction in accordance with the reviewer’s comments as detailed below (see Lines 46 to 110):

The available DEM studies in the literature have primarily investigated either the effect of initial fabric, *i.e.*, the inherent anisotropy on liquefaction resistance and cyclic response or, less frequently, the impact of Lode angle on the cyclic behavior of granular soils. However, the combined effect of the initial anisotropy and the anisotropy induced by the applied

stress remains mainly underexplored. For instance, Ajam Norouzi and Seyedi Hosseininia [1] highlighted the profound effect of initial fabric on cyclic liquefaction resistance through DEM modeling under biaxial compression tests. Their results confirm that varying fabric anisotropy affects the stress paths, leading to a significant decrease in the maximum internal friction angle. These observations align well with the triaxial undrained DEM results of [35, 38] where the profound dependency of cyclic liquefaction resistance of the samples on the choice of sample preparation technique and the orientation of bedding plane was reported. Focusing on microstructure evolution, Jiang et al. [13] performed cyclic triaxial DEM tests under drained conditions and validated a stress-force-fabric relationship that analytically correlates anisotropy with shear strength. The changes in inter-particle contact fabric during the liquefaction state of sand under triaxial cyclic loading were also investigated by Zhao et al. [39]. The study highlighted the advantages of directly tracing the path of fabric variations, providing a more intuitive representation of how induced anisotropy depends on the loading direction. In tandem with these studies, the pivotal role and induced effects of the rotation of the principal stress axis on the shear strength of granular soils under cyclic loading were also revealed by Iai et al. [11], Mo et al. [22]. Similarly, Wei et al. [34] conducted a series of undrained simple shear DEM simulations under unidirectional and multidirectional loading paths. Their findings revealed that granular soils exhibit significantly different liquefaction resistance depending on the loading conditions. Specifically, compared to unidirectional loading, granular packings are more prone to liquefaction under multidirectional loading paths. As previously discussed, further investigation is needed to understand the combined effects of inherent isotropy and load-induced anisotropy on liquefaction resistance and the undrained cyclic response, which is the focus of the current study. Two primary methodologies are mainly employed in DEM simulations to model the undrained behavior of fully saturated particulate media. The constant volume method (CVM) maintains volumetric strain invariance in particulate assemblies, while the second approach couples DEM with complementary numerical methods such as computational fluid dynamics (CFD) or Smoothed-particle hydrodynamic (SPH) to incorporate pore fluid effects. To enhance the computational efficiency, Liu et al. [18] coupled fluid methods (CFM) were developed to simulate particle-fluid interactions at the mesoscopic scale (e.g., [18, 26]). Significant advancements in this field include the pioneering work of Hakuno and Tarumi [9], who integrated Darcy's law with DEM to capture pore water pressure, and subsequent developments by researchers exploring various applications from biaxial testing of ellipsoid particles to 2D saturated granular materials. Salimi and Lashkari [29] introduced a DEM-CFM coupling scheme to model undrained responses in 3D anisotropic particulate assemblies. Multiple studies have validated the efficacy of this coupling scheme across diverse stress paths [12, 30–32]. Hence, the DEM-CFM coupling scheme is also employed to simulate the undrained response of particulate assemblies in this study.

REVIEWER A – 2. Other more specific comments: On page 11, we read "Under monotonic loading, [..] the discrepancy between the loading direction and the direction of the contact-normal-based fabric tensor gradually diminishes [..]. This conclusion is evident in the results presented in Figures 13, where increasing the Lode angle does not significantly affect the final values of the fabric components at the end of the shearing." This argument is, at best, confusing, as it relates direction of fabric in the Euclidean space to the Lode angle which is not Euclidean and is a measure of third invariant of stress.

Response:

Thank you very much for your valuable and constructive comment. Although the Lode angle is a scalar measure derived from the second and third invariants of the deviatoric stress tensor, it also has a geometric interpretation: it represents the clockwise angle from the major principal stress axis within the deviatoric (π) plane, often referred to as the octahedral plane (see Figure 2). On the other hand, the contact-normal-based fabric tensor, while defined in Euclidean space, can also be projected onto the same deviatoric (π) plane for meaningful comparisons with stress paths—particularly in the context of anisotropy evolution under different loading directions. We have previously demonstrated such directional fabric projections in the octahedral plane in Irani et al. [12]. In this context, our discussion of the alignment (or reduction in misalignment) between the loading direction and the evolving fabric orientation refers to their respective projections in the π-plane, making the interpretation consistent and physically meaningful. To clarify this point, we have added the following explanation in the revised manuscript (see Lines 713 to 723):

While the Lode angle is a scalar quantity derived from stress invariants, it has a geometric interpretation in the deviatoric (π) plane as the angle between the major principal stress direction and the loading path. The contact-normal fabric tensor, although formulated in Euclidean space, can also be projected onto the π-plane for comparison. Hence, the observed reduction in directional discrepancy between the loading direction and the fabric tensor during monotonic shearing is physically meaningful when viewed within this common projection framework.

REVIEWER A – 3. Following Equation 6, it is said that the fabric describes the "spatial distribution" of contacts. The authors mean "directional distribution". Spatial distribution is related to homogeneity/inhomogeneity while directional distribution is related to isotropy/anisotropy.

Response:

Thank you very much for this valuable comment. We have modified the text accordingly as:

In this context, **F** describes the directional distribution of contacts.

REVIEWER A – 4. On Eq 8, the authors need to clarify how rattlers are handled, specifically since a connection is made between coordination number and the transition between slid-like and liquid-like response. Incidentally, the threshold of CN=4 that has been mentioned on page 12 is not a correct assessment and there is a rich thread of studies on this threshold (beyond refs [7] and [9]). The authors are enticed to check the literature in physics community on the effect of parameters such as pressure and friction on jamming transition and the associated coordination number, e.g. https://doi.org/10.1039/C9SM01932D

Response:

Thank you very much for this insightful and constructive comment. We fully acknowledge that the jamming transition and associated coordination number are influenced by several factors, including pressure, friction, and particle shape (e.g., asphericity, aspect ratio). As rightly pointed out by the reviewer, a rich body of literature—particularly in the physics community—has investigated these dependencies extensively. From a physical and mechanical standpoint, however, the threshold coordination number of 4 holds foundational significance in three-dimensional granular assemblies. According to Maxwell's stability criterion, a minimum of four non-coplanar contacts is generally required to achieve mechanical stability for frictional particles. Below this threshold, particles retain excessive degrees of freedom, which undermines the structural rigidity of the assembly. As the coordination number increases beyond 4, translational and rotational constraints become more pronounced, and the energy required for particle rearrangement rises significantly. While we agree that the mechanical coordination number at the onset of liquefaction or transition to a fluid-like state can vary depending on particle characteristics—especially shape—our interpretation, based on available studies, is that this variation may not be substantial at the point of instability. Nevertheless, we recognize that this hypothesis requires further dedicated investigation. In our study, we therefore chose to report the mechanical coordination number—excluding rattlers—to focus specifically on load-bearing particles, which are more relevant to the mechanics of instability. We also added the following lines to the manuscript (see Lines 781 to 805):

Granular assemblies can exhibit fluid-like behavior with negligible static shear modulus. The MCN, which accounts only for force-bearing contacts (i.e., excluding rattlers), is primarily influenced by particle shape, interparticle friction, and confining pressure [17, 25, 33, 37]. For assemblies composed of spherical particles, a *coordination number* of CN = 4 is typically considered a critical threshold separating solid-like (CN ≥ 4) and liquid-like (CN < 4) behavior [5, 7]. When rattlers are excluded, the mechanical coordination number (MCN) provides a more refined measure of the load-bearing structure. Studies such as [36] suggest that the onset of liquefaction in spherical assemblies is characterized by MCN ≈ 3.6, while others report slightly lower thresholds—e.g., MCN = 3 [8] and MCN ≈ 2.8 [20].

However, in this study, due to the use of clumped, non-spherical particles, higher MCN values are observed at the onset of instability. Specifically, MCN ≈ 4.5 is reached across all assemblies during extension, which is considered indicative of the preliquefaction state. This is primarily due to shape-induced interlocking and enhanced contact stability, which delay the collapse of the contact network compared to spherical particles. Notable examples include studies on elliptical, concave, and polygonal particles, where coordination numbers remain above 4 under shear or dynamic conditions relevant to instability [2, 23].

Motivated by the reviewers' comment on rattlers and floaters, we have incorporated variations in MCN and the redundancy index that exclude rattlers from consideration. The following lines have been added to the manuscript (see Lines 236 to 242):

Figure 15 in the original manuscript (Figure 1 in the current document) and the following description, have been added to the manuscript (see Lines 806 to 819):

Figures 3(a–c) depict the variation of the mechanical coordination number (MCN) versus deviatoric strain under undrained cyclic loading for the TR0, TR45, and TR90 specimens sheared with $e_0 = 0.589$, $p'_0 = 100\,\text{kPa}$, and $\theta = 0^\circ$. As shown, the overall evolution of MCN is consistent across all three samples and qualitatively resembles the trend observed in the excess pore pressure evolution. Specimens with comparable initial void ratios show nearly identical MCN values at the onset of loading.

A comparison of Figures 3(a–c) reveals that the TR0 specimen reaches MCN ≈ 4.5 in fewer cycles compared to TR45 and TR90. This aligns with the macroscopic behavior discussed in Section 4, where a greater reduction in shear strength is observed in TR0 after approximately 60 cycles (see Figure 7). To further examine the evolution of the contact network, Figures 3(d–f) present the variation of the *redundancy index* I_R^f, which excludes floaters (particles with zero contacts). The redundancy index generally follows a similar trend to MCN, decreasing throughout the cyclic loading and converging toward unity, irrespective of initial fabric. These results are consistent with prior DEM studies [6, 20, 38, 41], which associate

the onset of liquefaction with a redundancy index approaching $I_R^f \approx 1$. Values of $I_R^f > 1$ indicate a solid-like, statically stable system, while $I_R^f < 1$ corresponds to a liquid-like, mechanically unstable state.

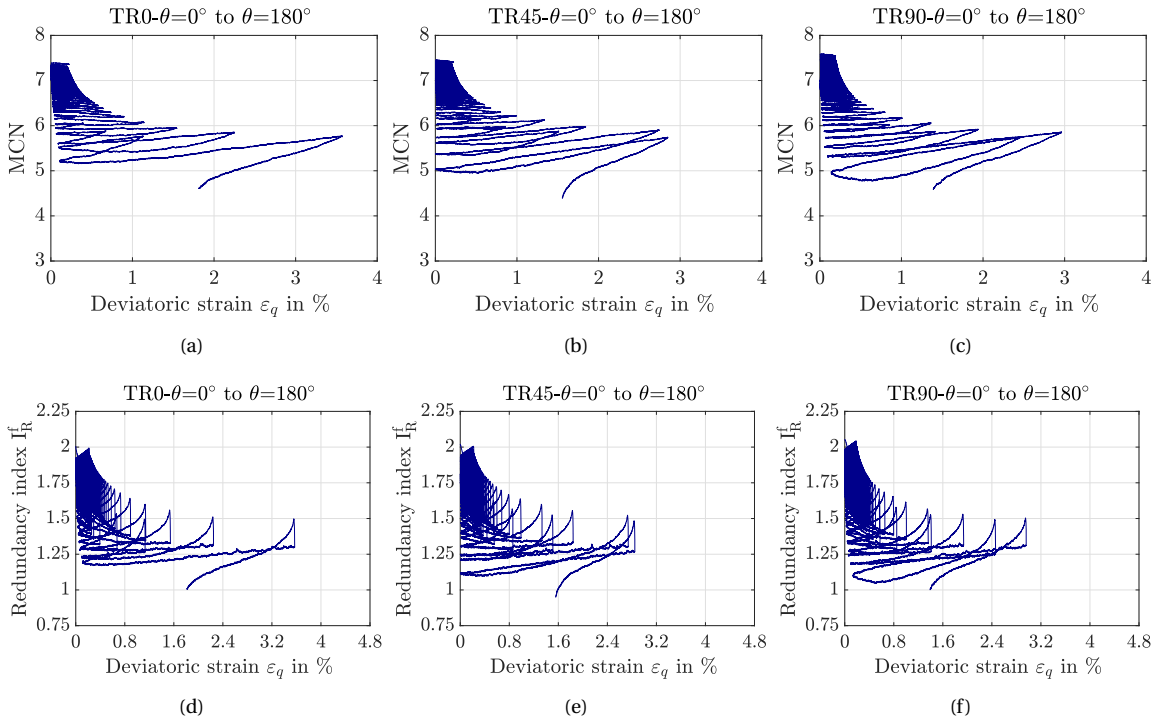

Figure 1: Variations of coordination number and redundancy index in semi-dense assemblies with $e_0 = 0.589$, $p'_0 = 100$ kPa sheared under the undrained true triaxial condition with $\theta = 0°$, (a & d): TR0; (b & e): TR45 and (c & f): TR90

REVIEWER A – 5. The damping ratio of 0.7 used in this study is too high and may have a non-negligible effect on CN at the phase transition.

Response:

Thank you for your insightful comment. In our simulations, the damping ratio is derived from the coefficient of restitution (CoR), which governs energy dissipation during particle collisions. For granular materials like sand, the CoR varies depending on the material properties and environmental conditions. Literature suggests that the CoR for dry rock or sand typically ranges from 0.3 to 0.6, while for wet conditions, it can be lower, ranging from 0.1 to 0.3 [14]. These CoR values correspond to damping ratios of approximately 0.2–0.3 for dry sand and 0.4–0.7 for wet sand, as the damping ratio is inversely related to the CoR. Given that our study simulates undrained cyclic loading conditions, where pore water is present, a damping ratio of 0.7 aligns with the upper bound of values reported for wet granular materials, reflecting the increased energy dissipation due to fluid-particle interactions. Regarding the potential effect on the coordination number at the phase transition, we acknowledge that the damping ratio can influence particle dynamics, particularly during cyclic loading where rearrangements occur. However, studies such as Zhou et al. [40] have demonstrated that damping ratios ranging from 0.1 to 0.8 have a negligible impact on macroscopic properties like the angle of repose, which is closely tied to particle coordination and packing stability. The coordination number at the phase transition—where the material transitions from solid-like to fluid-like behavior—is primarily governed by the stress state, Lode angle, and pore pressure evolution, as captured by our Coupled Fluid Method (CFM) simulations. The damping ratio primarily affects the rate of energy dissipation during individual particle contacts, but its influence on the overall coordination number is secondary compared to these macroscopic stress conditions. To further ensure the robustness of our results, we selected a damping ratio of 0.7 to conservatively account for the energy dissipation in wet, undrained conditions, consistent with prior DEM studies of saturated granular assemblies [3, 16]. While a sensitivity analysis was not conducted in this study due to computational constraints, the chosen value falls within the physically realistic range for our system, and we believe it does not significantly alter the coordination number trends reported. Nevertheless, we recognize the value of exploring damping ratio effects in future work and will consider conduct-

ing a sensitivity analysis to quantify its influence on phase transition behavior. The following description, have been added to the manuscript (see Lines 276 to 283):

In our simulations, a damping ratio of 0.7 is assumed to model energy dissipation under wet, undrained conditions. This value is reasonable for saturated granular materials, corresponding to a coefficient of restitution (CoR) of approximately 0.1–0.3, as reported for wet sand where fluid-particle interactions enhance energy loss [3], and aligns with damping ratios of 0.4–0.7 commonly used in DEM studies of wet systems [16].

REVIEWER A – 6. On page 6, the discussion resorts to the concept of force chains to interpret the stiffness of different samples. The relation between the details of the force chains and the stiffness is not immediately clear to me since, for a given contact, the stiffness remains fixed irrespective of the intensity of the contact force. At any rate, such discussions require visualizing the force chain.

Response:

Thank you very much for the constructive comment. The reviewer is absolutely correct. We have removed the following lines from the manuscript to avoid any confusion: "This phenomenon can be attributed to the orientation of force chains relative to particle geometry. In TR90 samples, force chains predominantly traverse the long axes of particles, whereas in TR0 samples, they pass through the shorter dimensions. Consequently, TR90 samples exhibit a more pronounced stiff behavior, necessitating a greater number of loading cycles to induce liquefaction."

REVIEWER A – 7. In Equation 9 a double log formula is suggested to empirically fit the data. Such compounding exponents introduce excessive sensitivities are generally avoided. Incidentally, correlating parameters with total deviatoric strain is fundamentally problematic as the latter is reference-dependent and therefore, the correlations are often not generalizable.

Response:

Thank you for your insightful feedback. We acknowledge the concerns regarding the use of the double logarithmic formulation in Equation 9. Our choice of this empirical approach was driven by its ability to accurately capture the observed experimental trends. However, we recognize that compounding exponents may introduce excessive sensitivity. To address this, we carefully considered alternative formulations that could offer a more stable representation. Nevertheless, Equation 9 remained our preferred choice, as it provided the best fit to the experimental data.

Regarding the correlation with total deviatoric strain, we recognize that it is reference-dependent, which could potentially limit the general applicability of the proposed correlation. Our intention was to provide a practical fit for the specific dataset under investigation, rather than a universally applicable model. Nonetheless, we added the reference deviatoric strain $\varepsilon^{acc}_{q,ref}$ defined for $\theta = 0^\circ$ at $G_{sec}/G^1_{sec} = 0.3$ to Eq. 9 as follows:

$$\frac{G_{sec}}{G^1_{sec}} = 30 \cdot \left(\exp\left(\frac{\varepsilon^{acc}_q}{\varepsilon^{acc}_{q,ref}} \right)^b \right)^c \tag{1}$$

We greatly appreciate your insightful comments and will incorporate them into our ongoing efforts to refine the proposed correlation.

REVIEWER A – 8. The manuscript attempts to correlate the different behaviour of the samples with the differences in their initial anisotropy. However, this anisotropy is clearly evolving (as is discussed towards the end of the manuscript). Therefore, it makes more sense to correlate the response at any given time to the current anisotropy. This becomes more meaningful to distinguish between the initial stages of tests, where the effect of the initial anisotropy is more obvious, with the later stages of the test where the contact anisotropy is becoming more aligned with stress.

Response:

Thank you very much for this thoughtful and important comment. We fully agree that fabric anisotropy evolves during shearing, and that the current fabric state has a direct influence on the macroscopic response. Indeed, many advanced constitutive models incorporate evolving fabric tensors to capture this behavior, as the evolving anisotropy affects both shear strength and volumetric response. However, our study specifically focuses on the role of initial fabric and load-induced anisotropy in shaping the response of granular assemblies. In undrained cyclic loading, particularly during the early stages, plastic strains—and thus fabric evolution—are relatively limited until the onset of liquefaction. Consequently, initial fabric anisotropy remains a dominant factor in governing the early mechanical response. This justifies our emphasis on initial fabric parameters, especially when distinguishing different sample behaviors during the pre-liquefaction phase. Moreover, while it is valuable to consider the current fabric state, in practice, only the initial state is typically accessible—especially for microstructural descriptors like fabric, which are difficult to measure even at the initial stage. Nevertheless, to acknowledge

the importance of evolving anisotropy, we include a detailed analysis of fabric development and its correlation with macro-scale response in Figure 13, capturing both the initial and evolving fabric components throughout the loading history.

REVIEWER A – 9. I cannot grasp the importance of the polynomial fits in Fig 8.
Response:
Thank you for this comment. The polynomial fits demonstrate that the relationship between the normalized shear modulus and the number of cycles can be effectively captured using a simple third-degree polynomial approximation. This approach aligns with the development of various empirical and explicit high-cycle accumulation models. Such polynomial approximations may prove valuable for deep learning-based approaches to predicting shear modulus evolution, once a sufficient number of experimental datasets are available. Additionally, they can serve as an initial estimation of the shear modulus for a given number of cycles and a specific Lode angle.

REVIEWER C – 1. This paper presents a DEM-CFD study focused on the cyclic behavior of granular assemblies with a focus on the effects of fabric and stress anisotropies. The methods used are robust, the results are interesting, and they make a strong contribution to the literature. Before recommending for publication, there are a number of comments that I would like to share with the authors:
One suggestion regarding the title is to add terms that relate to the fabric anisotropy, since apart from the stress anisotropy this is the major focus of the paper.
Response:
The authors would like to thank the reviewer for his/her time spent reviewing the manuscript and for providing valuable comments and information. To address this comment, we have changed the title of the manuscript to the following:

Micromechanical Influence of Fabric Anisotropy and Stress Path Dependency on Liquefaction Susceptibility in Granular Soils

REVIEWER C – 2. Sentence on the bottom left column of page 2 saying "This approach might be time-consuming and may not account for excess pore water pressure resulting from volume strain" – could you provide additional information regarding what this sentence specifically refer to?
Response:
Thank you very much for this constructive comment. We were referring to the fact that the CFD coupling approach employs the locally volume-averaged Navier-Stokes equations to simplify the flow field and might be computationally demanding. We agree with the reviewer that the sentence structure led to some misunderstanding. Motivated by the reviewers's suggestion, we have revised this section of the manuscript, which is now clarified as follows (see Lines 88 to 110):

Two primary methodologies are mainly employed in DEM simulations to model the undrained behavior of fully saturated particulate media. The constant volume method (CVM) maintains volumetric strain invariance in particulate assemblies, while the second approach couples DEM with complementary numerical methods such as computational fluid dynamics (CFD) or Smoothed-particle hydrodynamic (SPH) to incorporate pore fluid effects. To enhance the computational efficiency [18], coupled fluid methods (CFM) were developed to simulate particle-fluid interactions at the mesoscopic scale (e.g., [18, 26]). Significant advancements in this field include the pioneering work of [9], who integrated Darcy's law with DEM to capture pore water pressure, and subsequent developments by researchers exploring various applications from bi-axial testing of ellipsoid particles to 2D saturated granular materials. [29] introduced a DEM-CFM coupling scheme to model undrained responses in 3D anisotropic particulate assemblies. Multiple studies have validated the efficacy of this coupling scheme across diverse stress paths [12, 30–32]. Hence, the DEM-CFM coupling scheme is also employed to simulate the undrained response of particulate assemblies in this study.

REVIEWER C – 3. Regarding the same section as the previous comment, can you add more information regarding the benefits of using CFD coupling in DEM simulations over using the constant volume approximation?
Response:

Thank you very much for this comment. The selection of the CFM over the constant volume method was driven by several key considerations. First, as mentioned in the manuscript as a reply to the previous comment, CFM provides a more physically representative simulation of undrained conditions by explicitly modeling the fluid-particle interactions. More importantly, the nature of our stress-controlled loading conditions made CFM the more appropriate choice. When performing stress-controlled tests, maintaining truly undrained conditions using the constant volume method presents significant

challenges. This is because the constant volume method enforces undrained behavior through volume constraints, which can conflict with the imposed stress boundary conditions. when the Lode angle is set to 30°, CVM fails to maintain a constant Lode angle during undrained monotonic loading. For strain-controlled loading to simulate a Lode angle of 30°, two conditions must be met:

1. **No volumetric strain:**
$$V_x(yz) + V_y(xz) + V_z(xy) = 0$$
where V_x, V_y, and V_z are the boundary velocities in the x, y, and z directions, respectively, and x, y, z are the dimensions of the domain.

2. **Intermediate principal stress ratio condition:** For $b = \frac{\sigma_y - \sigma_x}{\sigma_z - \sigma_x} = 0.5$ (where z is the major principal stress direction), the coaxiality condition requires:
$$0.5V_z + 0.5V_x = V_y$$

Solving these equations yields the velocity ratios required to maintain a constant Lode angle. However, in practice, such precise velocity control is difficult to achieve using CVM, and the resulting stress path deviates from the intended Lode angle. As demonstrated in Fig. 2, CVM fails to reproduce the desired stress path at 30° Lode angle under undrained conditions.

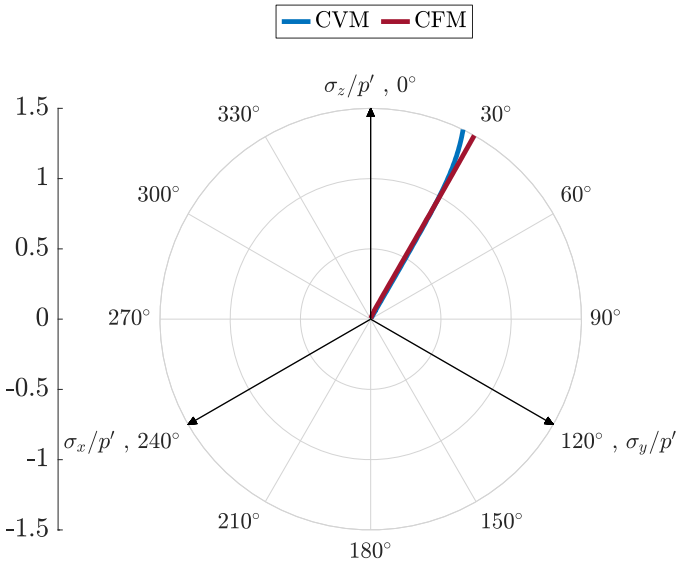

Figure 2: Comparison of CFM and CVM under monotonic undrained loading at a Lode angle of 30°.

To address the reviewer's comment, we have added the following lines to the manuscript (see Lines 151 to 155):

Given the stress-controlled nature of the applied loading and stress-strain non-coaxialilty under true triaxial loading scenarios, the commonly used constant volume approach was deemed inappropriate for the purpose of this study.

REVIEWER C – 4. Last sentence of section 1: what does "its" refer to specifically in this sentence?
Response:
Thank you very much for this comment. We have modified the text as follows (see Lines 131 and 132):

Lastly, the numerical description of the secant shear modulus is discussed.

REVIEWER C – 5. Could you explain the reason for using the coordination number instead of the mechanical coordination number or particle connectivity, particularly since studies have shown that the latter parameters are more strongly correlated with the material's mechanical response?
Response:
Thank you very much for this comment. We didn't provide MCN = $\frac{2N_c - N_p^1}{(N_p - N_p^0 - N_p^1)}$ because on that time our code only calculated

N_p^0 (floater particles with zero contacts) and not N_p^1. Given the substantial computational time required for each simulation (approximately 24 days), recalculating to include N_p^1 took time within the review timeframe. To address the reviewers' comment, we have incorporated variations in the redundancy index and Mechanical Coordination Number (MCN) that exclude rattlers from consideration. The following lines have been added to the manuscript (see Lines 236 to 242):

The MCN and redundancy index I_R^f defined as:

$$\text{MCN} = \frac{2N_c - N_p^1}{N_p - N_p^0 - N_p^1} \; ; \; I_R^f = \frac{(3-2f_s)N_c}{6(N_p - N_p^0)} \tag{2}$$

where N_p is the total number of particles. N_p^0 denotes the count of floating particles that have no contacts. The sliding fraction, f_s, measures the percentage of slipping contacts in granular assemblies, expressed as the ratio of sliding contacts to the total active contacts.

Figure 15 in the original manuscript (Figure 3 in the current document) and the following description, have been added to the manuscript (see Lines 772 to 819):

Figures 3(a–c) depict the variation of the mechanical coordination number (MCN) versus deviatoric strain under undrained cyclic loading for the TR0, TR45, and TR90 specimens sheared with $e_0 = 0.589$, $p_0' = 100\,\text{kPa}$, and $\theta = 0^\circ$. As shown, the overall evolution of MCN is consistent across all three samples and qualitatively resembles the trend observed in the excess pore pressure evolution. Specimens with comparable initial void ratios show nearly identical MCN values at the onset of loading.

Granular assemblies can exhibit fluid-like behavior with negligible static shear modulus. The MCN, which accounts only for force-bearing contacts (i.e., excluding rattlers), is primarily influenced by particle shape, interparticle friction, and confining pressure [17, 25, 33, 37]. For assemblies composed of spherical particles, a *coordination number* of CN = 4 is typically considered a critical threshold separating solid-like (CN ≥ 4) and liquid-like (CN < 4) behavior [5, 7]. When rattlers are excluded, the mechanical coordination number (MCN) provides a more refined measure of the load-bearing structure. Studies such as [36] suggest that the onset of liquefaction in spherical assemblies is characterized by MCN ≈ 4, while others report slightly lower thresholds—e.g., MCN = 3 [8] and MCN = 3.2 [20].

However, in this study, due to the use of clumped, non-spherical particles, higher MCN values are observed at the onset of instability. Specifically, MCN ≈ 4.5 is reached across all assemblies during extension following compression, which is considered indicative of the preliquefaction state. This finding is supported by studies such as [38] and [36], which also report MCN values greater than 4 for non-spherical particles prior to liquefaction.

A comparison of Figures 3(a–c) reveals that the TR0 specimen reaches MCN ≈ 4.5 in fewer cycles compared to TR45 and TR90. This aligns with the macroscopic behavior discussed in Section 4, where a greater reduction in shear strength is observed in TR0 after approximately 60 cycles (see Figure 7). To further examine the evolution of the contact network, Figures 3(d–f) present the variation of the *redundancy index* I_R^f, which excludes floaters (particles with zero contacts). The redundancy index generally follows a similar trend to MCN, decreasing throughout the cyclic loading and converging toward unity, irrespective of initial fabric. These results are consistent with prior DEM studies [6, 20, 38, 41], which associate the onset of liquefaction with a redundancy index approaching $I_R^f \approx 1$. Values of $I_R^f > 1$ indicate a solid-like, statically stable system, while $I_R^f < 1$ corresponds to a liquid-like, mechanically unstable state.

REVIEWER C – 6. Could additional discussion be provided regarding what material is the simulated granular assembly intending to represent with regards to its particle shape, size, and gradation? For example, is the behavior intended to reproduce that of a specific clean sand?

Response:

Thank you for your insightful comment. In this study, we are not replicating a specific sand from the literature. However, since the primary focus is to evaluate liquefaction potential, we have selected a poorly graded sand. This choice is guided by established research demonstrating that poorly graded sands are more susceptible to liquefaction than well-graded sands [10, 27]. According to established literature, such as Mitchell and Soga (2005, Fundamentals of Soil Behavior, page 88) [21], the aspect ratio generally ranges from approximately 1.0 to 1.5 for sand particles. In contrast, silt particles, which tend to be more elongated, exhibit aspect ratios ranging from about 1.5 to 3.0. Mitchell and Soga further report that, across a broad dataset of soil particles, the mean aspect ratio is approximately 1.4, while the median value is 1.8. In our study, we opted to use an aspect ratio of 1.8:1, corresponding to the median value, for several reasons. First, the median provides a representative measure of central tendency that better reflects the typical particle morphology in a heterogeneous soil

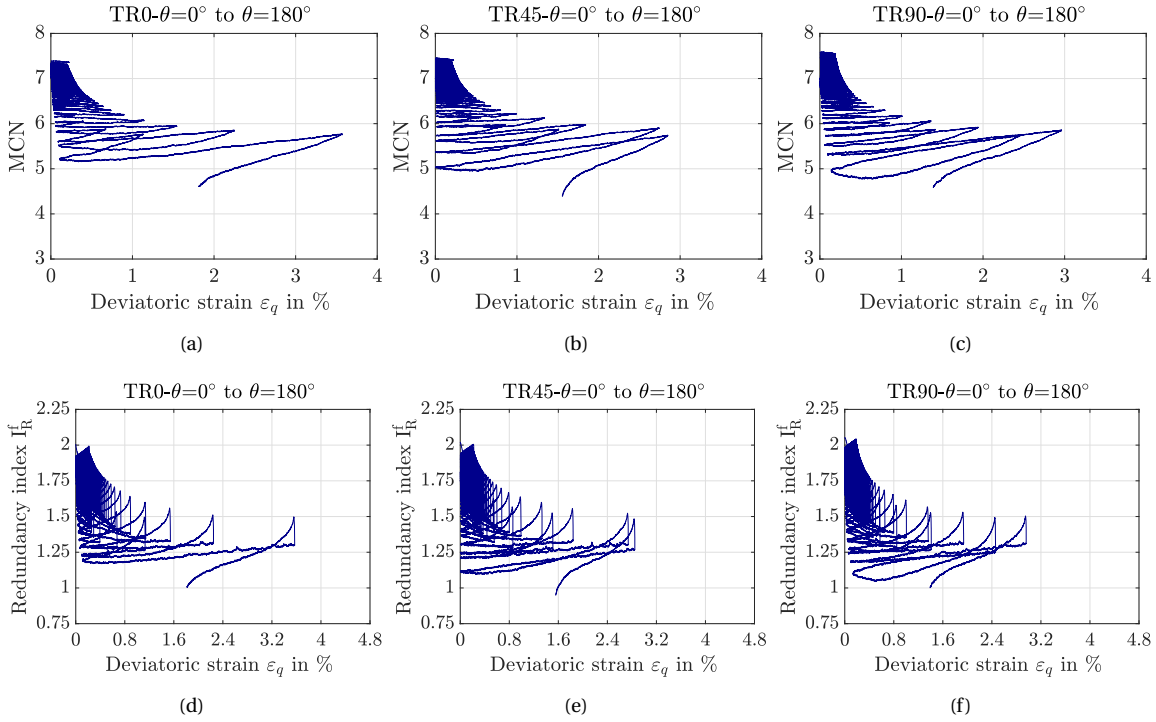

Figure 3: Variations of coordination number and redundancy index in semi-dense assemblies with $e_0 = 0.589$, $p'_0 = 100$ kPa sheared under the undrained true triaxial condition with $\theta = 0°$, (a & d): TR0; (b & e): TR45 and (c & f): TR90

assembly, as it is less influenced by extreme values compared to the mean. This is particularly relevant for our DEM-CFM simulations, where we aim to model a realistic yet generalized representation of anisotropically consolidated granular soils under cyclic loading. An aspect ratio of 1.8:1 falls within the upper range of sand particles and the lower range of silt particles, making it a reasonable compromise that captures the transitional behavior of granular soils commonly encountered in practice. Additionally, the choice of 1.8:1 aligns with the objectives of our study, which focus on understanding the influence of particle-scale properties on macroscopic undrained behavior under varying Lode angles. By selecting the median value from the literature, we ensure that our simulations are grounded in a statistically defensible baseline that reflects typical soil conditions, as opposed to an arbitrary or outlier value.

To address the reviewer's comment, the following lines have been added to the manuscript (see Lines 262 to 265):

A poorly graded sand, characterized by a coefficient of uniformity ($C_u = 1.5$) and a coefficient of curvature ($C_c = 1.02$), is selected due to its higher susceptibility to liquefaction compared to well-graded sands [10, 27].

REVIEWER C – 7. Related to the point above, it would be beneficial to include some data showing the ability of the DEM-CFM model to reproduce typical behaviors of granular materials, like stress dependency, stress dilatancy, and critical states. This could be addressed by including a section on parameter calibration.

Response:

Thank you very much for this insightful comment. The ability of the proposed DEM-CFM coupling scheme to capture key aspects of granular material behavior, including stress dependency, dilatancy, and critical state, has been validated in our previous work published in [12, 29]. In the present study, we did not recalibrate the DEM model using experimental data; instead, we adopted the same set of parameters from our previous work to specifically focus on the cyclic response. To address the reviewer's concern, we have included monotonic simulations under both drained (see Fig. 4) and undrained (see Fig. 5) conditions using the DEM-CFM coupling scheme as examples. In [12], approximately 700 monotonic tests were simulated, and a deep-learning-based approach was proposed for fabric quantification. Additionally, in [29], the DEM-CFM coupling scheme was introduced, with evaluations of dilatancy, fabric evolution, and critical state properties. Moreover, both studies included comparisons between simulation results and experimental data.

REVIEWER C – 8. Could a reference be provided to put the void ratio value in context? For example, a state parameter or

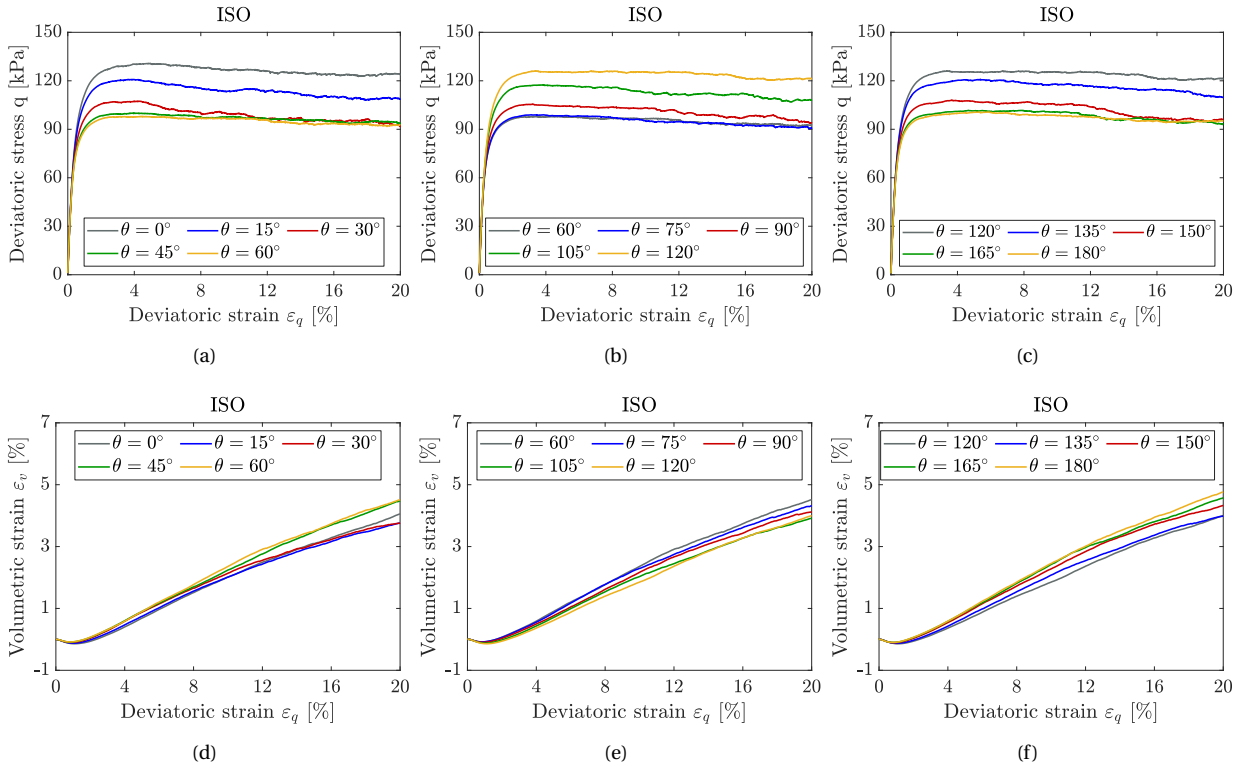

Figure 4: Mechanical response of medium-dense isotropic (ISO) assemblies with $e_0 = 0.589$, $p'_0 = 100$ kPa under drained true triaxial condition for a & d: $\theta = 0°$ to $60°$, b & e: $\theta = 60°$ to $120°$, c & f: $\theta = 120°$ to $180°$

relative density would provide such context.
Response:

Thank you very much for this constructive comment. We have added the value of relative density to the manuscript. All simulations are conducted on medium-dense assemblies with a relative density of $D_r \approx 0.55$ and initial void ratio of $e_0 \approx 0.590$.

REVIEWER C – 9. Regarding the selection of the linear contact model, could the authors add some context related to the ability of this model to reproduce granular material behavior considering that the effective stress in the simulations is changing from the initial value of 100 kPa to close to zero in a liquefied state? This would cause a change in the stiffness in contacts in real granular materials, which is not considered by the linear contact model.
Response:
We thank the reviewer for this insightful comment. We acknowledge that the linear contact model does not account for stress-dependent contact stiffness, and thus cannot fully capture the nonlinear elastic behavior of real granular contacts, especially under varying effective stress conditions such as those encountered during liquefaction. However, the main objective of our study is to investigate the influence of fabric anisotropy and Lode angle on the macroscopic manifestation of liquefaction rather than to reproduce contact-level mechanical responses with high fidelity. The linear contact model was chosen for its computational efficiency and its widespread use in similar DEM studies. While it assumes constant normal and tangential stiffness, our calibrated model was still able to reproduce key features of undrained cyclic loading, such as pore pressure buildup, strength degradation, and large deformations. We argue that these macroscopic responses are sufficiently captured for the purpose of our study. To acknowledge this limitation, we have added the following sentence in the revised manuscript (see Lines 271 to 276):

Nonlinear contact models, such as the Hertz-Mindlin model, can represent stress-dependent stiffness more realistically, but were not adopted in this study due to their higher computational cost and the adequate performance of the calibrated linear model in capturing the observed liquefaction phenomena.

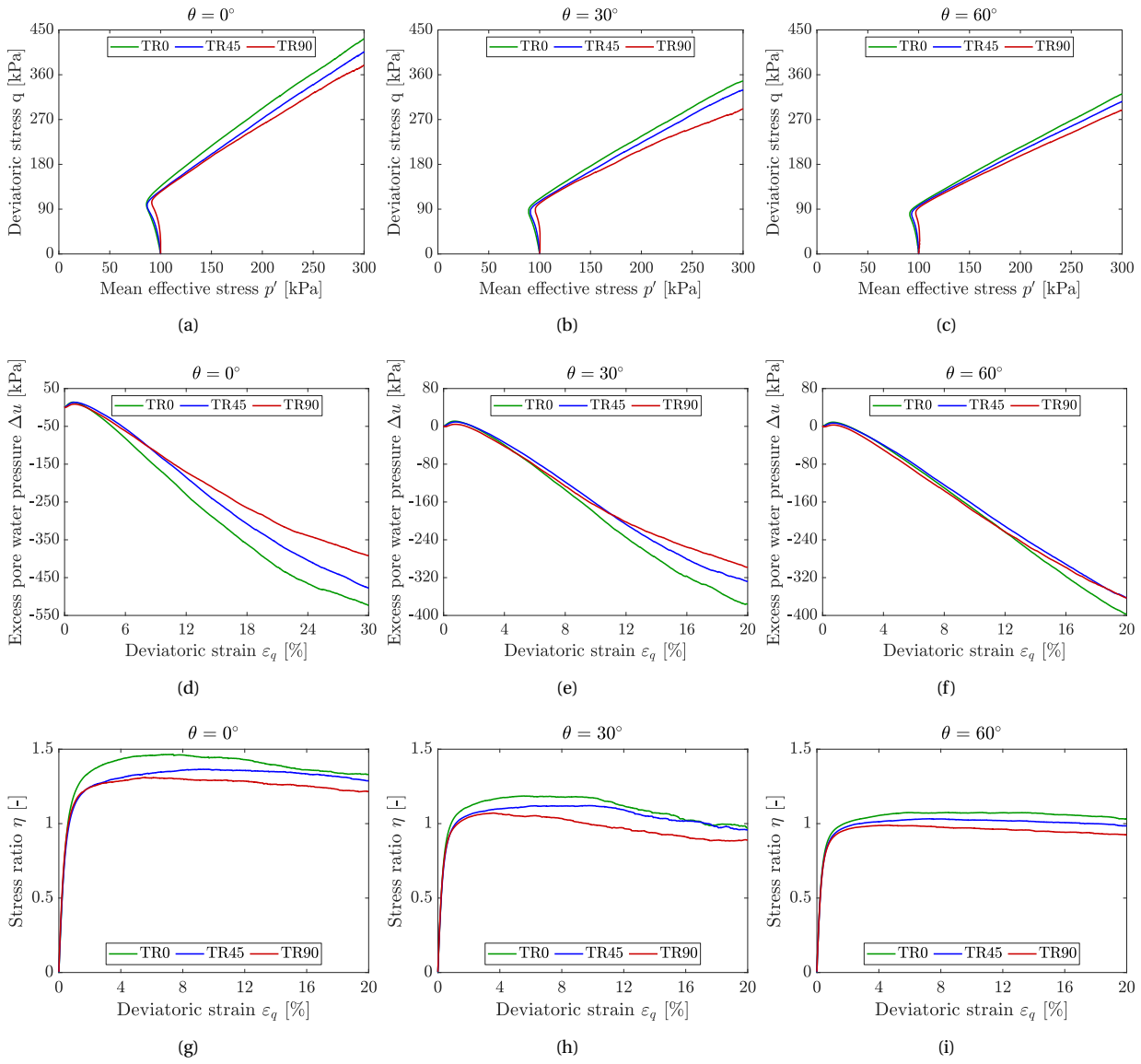

Figure 5: The effect of initial fabric on the mechanical response of medium-dense assemblies sheared under the undrained condition and (a),(d) & (g): $\theta = 0°$, (b),(e) & (h): $\theta = 30°$ and (c),(f) & (i): $\theta = 60°$ in $p' - q$, $\varepsilon_q - \Delta u$ and $\varepsilon_q - \eta$ plane

REVIEWER C – 10. A damping ratio of 0.7 is higher than typically used in DEM simulation. Could the authors provide information regarding the need to use of such a high value?

Response:

Thank you for your insightful comment. In our simulations, the damping ratio is derived from the coefficient of restitution (CoR), which governs energy dissipation during particle collisions. For granular materials like sand, the CoR varies depending on the material properties and environmental conditions. Literature suggests that the CoR for dry rock or sand typically ranges from 0.3 to 0.6, while for wet conditions, it can be lower, ranging from 0.1 to 0.3 [14]. These CoR values correspond to damping ratios of approximately 0.2–0.3 for dry sand and 0.4–0.7 for wet sand, as the damping ratio is inversely related to the CoR. Given that our study simulates undrained cyclic loading conditions, where pore water is present, a damping ratio of 0.7 aligns with the upper bound of values reported for wet granular materials, reflecting the increased energy dissipation due to fluid-particle interactions. Regarding the potential effect on the coordination number at the phase transition, we acknowledge that the damping ratio can influence particle dynamics, particularly during cyclic loading where rearrangements occur. However, studies such as Zhou et al. [40] have demonstrated that damping ratios ranging from 0.1 to 0.8 have a negligible impact on macroscopic properties like the angle of repose, which is closely tied to particle coordination and packing stability. The coordination number at the phase transition—where the material transitions from solid-like to fluid-like behavior—is primarily governed by the stress state, Lode angle, and pore pressure evolution, as captured by our Coupled Fluid Method (CFM) simulations. The damping ratio primarily affects the rate of energy dissipation during individual particle contacts, but its influence on the overall coordination number is secondary compared to these macroscopic stress conditions. To further ensure the robustness of our results, we selected a damping ratio of 0.7 to conservatively account for the energy dissipation in wet, undrained conditions, consistent with prior DEM studies of saturated granular assemblies [3, 16]. While a sensitivity analysis was not conducted in this study due to computational constraints, the chosen value falls within the physically realistic range for our system, and we believe it does not significantly alter the coordination number trends reported. Nevertheless, we recognize the value of exploring damping ratio effects in future work and will consider conducting a sensitivity analysis to quantify its influence on phase transition behavior. The following description, have been added to the manuscript (see Lines 276 to 283):

In our simulations, a damping ratio of 0.7 is assumed to model energy dissipation under wet, undrained conditions. This value is reasonable for saturated granular materials, corresponding to a coefficient of restitution (CoR) of approximately 0.1–0.3, as reported for wet sand where fluid-particle interactions enhance energy loss [3], and aligns with damping ratios of 0.4–0.7 commonly used in DEM studies of wet systems [16].

REVIEWER C – 11. Please include information regarding the criterion used to finish a given simulation. Is a given number of cycles applied, or is there a target ru or deviatoric strain?

Response:

All tests were terminated once the normalized excess pore water pressure reached $r_u = 0.99$.The following lines have been added to the manuscript (see Lines 362 to 363):

All tests are terminated once the normalized excess pore water pressure reaches $r_u = 0.99$.

REVIEWER C – 12. Please describe how the deviatoric strain is calculated.

Response:

Thank you so much for your valuable comment, the following lines are included in the manuscript (see Lines 188 to 191):

Deviatoric strain (ε_q) can be calculated as follows:

$$\varepsilon_{\mathrm{q}} = \sqrt{\frac{2}{9}\left[(\varepsilon_1 - \varepsilon_2)^2 + (\varepsilon_2 - \varepsilon_3)^2 + (\varepsilon_3 - \varepsilon_1)^2\right]} \tag{3}$$

which ε_i (i=1, 2 and 3) is strain along direction i.

REVIEWER C – 13. Please include the shearing rate used in the simulation and quantification of inertial numbers to indicate whether the tests are performed in quasi-static conditions.

Response:

Thank you very much for this comment. To ensure quasi-static loading conditions, the applied shear strain rate was kept below 5×10^{-5} s^{-1}, in accordance with the criterion proposed by Kuhn [15]. Additionally, the simulations satisfied the inertial number criterion, maintaining $I < 0.001$ as recommended by Lopera Perez et al. [19]. Lines 330 to 342 are added to address the reviewer's comment:

The inertial effects were characterized using the inertial number I, defined as [28]:

$$I = \frac{\dot{\gamma} d}{\sqrt{p/\rho}} \tag{4}$$

where $\dot{\gamma}$ is the shear strain rate, d is the particle diameter, p is the confining pressure, and ρ is the particle density. The inertial number I quantifies the ratio of inertial to confining forces, providing a measure of the dynamic regime of the granular assembly. A shear strain rate of 5×10^{-5}s^{-1} and a time step of 1.5×10^{-7}s were employed in the simulations. These parameters result in an inertial number of approximately 0.0003 at the onset of loading, confirming that the simulations remain within the quasi-static regime throughout the deformation process.

REVIEWER C – 14. Please provide a more detailed description of the way in which the samples are sheared. For instance, what amplitude of deviator stress is applied to the samples? How do the individual stresses change during a simulation? Why are the deviatoric strains always positive? I would have expected them to be negative on the extension side. This could be addressed by including a figure showing how the three stress and strain components vary during an entire simulation. This point caused confusion for me as I read the paper.
Response:
We appreciate the reviewer's detailed comment. We have revised the manuscript to include a more comprehensive description of the shearing procedure, including how stress components are calculated and interpreted. The following paragraph has been added to the manuscript (see Lines 298 to 323):

The loading was applied in the z-direction by moving the boundaries at a constant velocity to impose a controlled z-axial strain. To maintain a constant mean stress and specified Lode angle during cyclic loading, a servo-controlled algorithm was employed. At each time step, the z-axial stress component was measured, and using the Lode angle definition and the constant mean stress condition, the lateral stress components in the x- and y-directions were calculated and adjusted accordingly. The pore pressure was computed using the CFM, and the corresponding effective stresses were used to control the applied boundary forces. In the post-processing stage, deviatoric stress, q, was calculated from the general formulation based on principal stress differences. While q is strictly a positive scalar by definition, we assign a negative sign to q during extension by referencing the direction of the stress path relative to the hydrostatic axis in the octahedral stress plane. This sign convention allows us to consistently distinguish between compression and extension phases, even though true tensile (negative) stresses are not present in the DEM simulation, as interparticle forces remain compressive unless cohesive models are used. Once the deviatoric stress q^{amp} reached 50 kPa during loading, the direction of loading was reversed to simulate unloading, and this process was repeated cyclically to maintain controlled stress amplitudes in both compression and extension phases.

We also note that in DEM simulations of cohesionless granular materials, stresses are emergent and inherently compressive. Therefore, the concept of "negative" stress (in tension) is not applicable in the traditional sense. Instead, extension is represented by the relative magnitudes of principal stresses, and q becomes negative by convention when the major principal stress is lateral. While we considered adding a figure showing the evolution of all stress and strain components, we found it would not resolve this misunderstanding, as no principal stress becomes negative; only their relative differences change direction. We hope this clarification sufficiently resolves the confusion.

REVIEWER C – 15. Please define the stress ratio.
Response:

Thank you very much for this comment. The stress ratio has been defined as follows:

Figure 3 shows the variations of stress ratio $\eta = q/p'$ versus deviatoric strain ε_q.

REVIEWER C – 16. Regarding the sentence on page 6 saying "This phenomenon can be attributed to the orientation of

force chains relative to particle geometry. In TR90 samples, force chains predominantly traverse the long axes of particles, whereas in TR0 samples, they pass through the shorter dimensions. Consequently, TR90 samples exhibit a more pronounced stiff behavior, necessitating a greater number of loading cycles to induce liquefaction" – this sentence describes the resulting observation. Could the authors provide discussion regarding the cause for this? i.e., why does having the force chains transversing the particle long axes results in additional stability?

Response:

Thank you very much for the constructive comment. We agree with the reviewer that the cause of this behavior requires further clarification and that additional evidence on force chain orientation would strengthen the argument. In response to Reviewer A's suggestion, we have removed the original speculative statement from the manuscript to avoid confusion. However, we would like to elaborate here on the underlying mechanical rationale. In samples composed of elongated particles, the orientation of particles relative to the loading direction can significantly affect the stability of force chains. In the TR90 samples, particles are aligned such that their long axes are oriented along the vertical loading direction (z-axis). This alignment allows force chains to form along the most mechanically stable axis of the particles. Since the particles are rigid and elongated, axial loading along their longer dimensions is less prone to force chain buckling, resulting in a stiffer response and delayed onset of liquefaction. In contrast, in the TR0 samples, the elongated particles lie primarily in the horizontal (x–y) plane, while the major principal stress is applied vertically. As a result, the force chains form through the shorter axes of the particles. This configuration is inherently less stable under axial compression, making the force chains more susceptible to buckling and collapse. This increased instability facilitates earlier pore pressure buildup and a more rapid progression toward liquefaction. We hope this explanation clarifies the cause behind the observed behavior and provides a clearer mechanical basis for the influence of particle orientation on liquefaction resistance.

REVIEWER C – 17. Regarding the sentence on page 6 saying "A reduction in Gsec can lead to greater strain accumulation, which may, in turn, cause increased pore water pressure due to the constant volume constraint" – I'm curious about the cause and effect relationship. The sentence indicates that a reduction in Gsec leads to pore water pressure. Couldn't the relationship be the opposite? i.e. as pore pressures increase the Gsec decreases as a result of decreasing effective stress. Additional discussion would be appreciated.

Response:

Thank you very much for bringing this to our attention. The reviewer is absolutely right in highlighting the need to clarify the causal relationship. In our original sentence, the direction of cause and effect was not accurately represented. We agree that the primary driver is the buildup of excess pore water pressure, which reduces the effective stress and, consequently, the shear stiffness G_{sec}. To further clarify, during undrained cyclic loading, the initial response involves a tendency for volumetric contraction or dilation depending on the loading direction and fabric. Under undrained conditions, this volumetric tendency cannot be realized, and instead results in the generation of excess pore pressure. As pore pressure increases, the effective mean stress decreases. This reduction in effective stress lowers the material stiffness, including G_{sec}, and enables further strain accumulation. At large strains, this process may accelerate as shear modulus further degrades due to both stress-path effects and material softening. We appreciate the reviewer's insight, which helped us improve the clarity and correctness of the physical interpretation. Accordingly, we have revised the sentence in the manuscript as follows (see Lines 573 to 575):

An increase in pore water pressure under constant volume conditions can lead to a reduction in G_{sec}, which, in turn, may accelerate strain accumulation.

REVIEWER C – 18. Regarding the sentence on page 6 saying "It is also evident that samples with bedding planes parallel to the major principal applied stress exhibit higher stiffness under identical strain levels and loading conditions" – it is not possible to see the higher stiffness because the results are provided in normalized form, which highlight the rate of degradation but not the relative stiffness magnitudes. Could the results also be presented in absolute form?

Response:

Thank you very much for your insightful comment. We agree with the reviewer that presenting stiffness data only in normalized form emphasizes degradation trends but does not convey the absolute magnitudes of stiffness, which are essential for interpreting relative material behavior. The original sentence was intended to refer to the relative degradation behavior, not the absolute stiffness values. However, we recognize that the phrasing may have caused confusion. To clarify this point and respond to the reviewer's suggestion, we have added a new figure (Figure 6 in the manuscript) to the manuscript, which presents the absolute values of secant shear modulus during the first loading cycle for all tested configurations. We have also revised the manuscript wording accordingly to distinguish between initial stiffness and degradation behavior more clearly. Figure 6 and the following lines have been added to the manuscript (see Lines 516 to 530):

Figure 6 illustrates the variation of G^1_{sec} under different Lode angles for the TR0, TR45, and TR90 assemblies. It is evident that

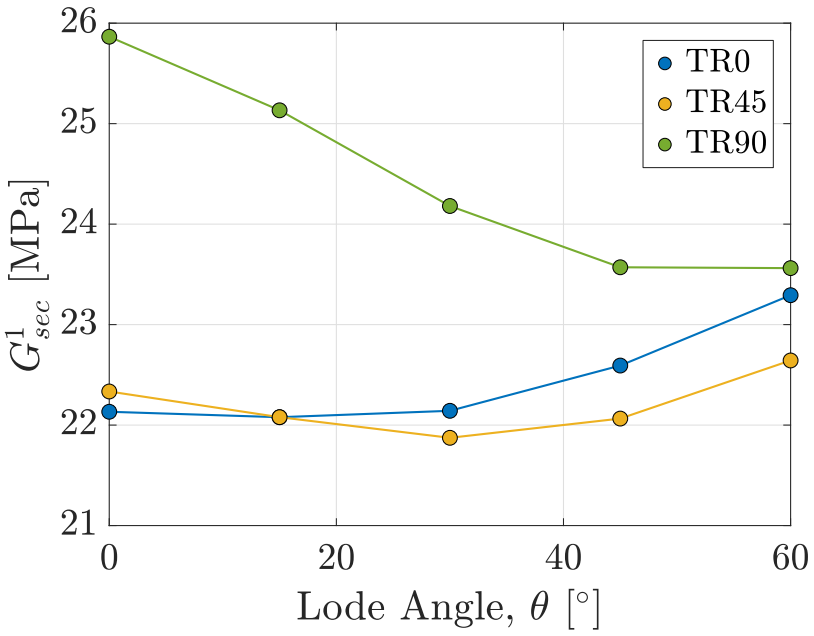

Figure 6: Variation of secant shear modulus during the first loading cycle for samples with different bedding plane orientations under various Lode angles.

under $\theta = 0°$, the TR90 samples exhibit the highest initial secant shear modulus, while the TR0 samples display the lowest. For TR0, an increasing trend in G^1_{sec} is observed as the Lode angle increases, whereas TR90 shows a decreasing trend over the same range. Interestingly, TR45 initially exhibits a reduction in G^1_{sec} up to $\theta = 30°$, followed by an increasing trend toward $\theta = 60°$. At $\theta = 60°$, the TR0 and TR90 samples converge to similar G^1_{sec} values. This convergence may be attributed to the fact that both assemblies are in an extension-dominated regime, where the bedding planes are approximately aligned with the major principal stress direction—resulting in comparable mechanical constraints regardless of initial anisotropy.

REVIEWER C – 19. First line on right column of page 9 – should it say an angle of 0 degrees of TR0 and TR90?
Response:
Thank you very much for bringing this point to our attention. We have revised the text accordingly as follows (see Lines 627 to 630):

For TR0 and TR90 samples, the highest resistance to deformation is exhibited under a loading direction of $\theta = 0°$, whereas for TR45, the greatest stiffness is achieved along loading paths with $\theta = 60°$.

REVIEWER C – 20. Regarding Section 5.1 – are the trends in fabric evolution the same of TR45 and TR90 samples? Since the results of these are not presented, the insights of this section are limited to the effect of stress anisotropy.
Response:

Thank you very much for this comment. Since the qualitative trend of changes in the fabric components under different Lode angles remained consistent, we did not include all the figures in the manuscript for the sake of brevity. Moreover, this section focuses specifically on the anisotropy induced by the applied load rather than inherent anisotropy.

REVIEWER C – 21. Could the prediction included in Fig. 10 be included in Fig. 6 to show the quality of the fit?
Response:
Thank you very much for this constructive suggestion. We have merged Figures 10 and 6 according to the reviewer's comment. The updated figure is as follows :

REVIEWER C – 22. Sentence on page 10 saying "For instance, Figures 13(a) and (b) show a decrease in Fx and Fy beyond a deviatoric strain level of q=3.4%", what does a strain "beyond" 3.4% refer to, since the maximum strain in the figure is 3.4%?

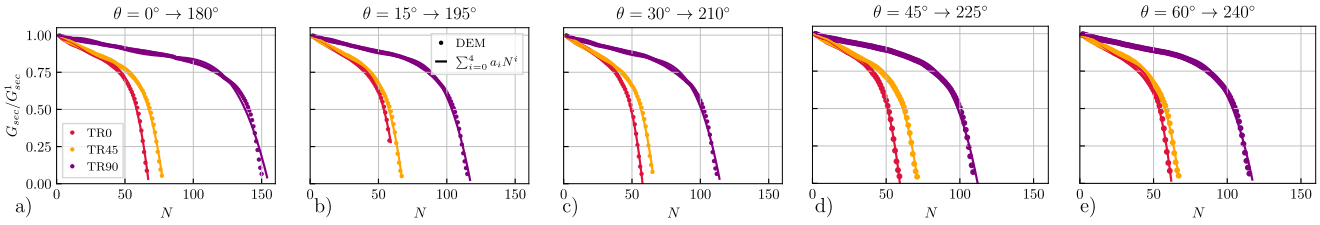

Figure 7: Approximation of secant shear modulus curve via $G_{sec}/G^1_{sec} = \sum_{i=0}^{4} a_i N^i$. The dots represent the DEM results, while the solid lines depict the numerical approximations.

Response:
Thank you very much for your comment. In these lines, we are referring to the quarter of the last cycle in the figures. We have revised the sentence as follows (Lines 694 to 701):

Considering the last fourth of the cycle in Figures 13 (a) and (b), where the deviatoric strain level decreases from ε_q=3.4% to ε_q=1.7%, F_x and F_y decrease from 0.355 to 0.3. This decline suggests a reduction in contacts along the x and y loading directions. In contrast, F_z increases from 0.27 at ε_q = 3.4% to 0.4 at ε_q = 1.7%, indicating the establishment of new contacts and changes in inter-particle interactions along the z direction.

REVIEWER C – 23. Can you please provide further discussion on the sentence on page 12 saying "These observations align with the results shown in Figures 3(a), (b), and (c), where the maximum stress ratio for TR0 samples is attained at a lower "q compared to TR45 and TR90 samples"?
Response:
Thank you very much for this constructive comment. To address the reviewer's concern, we have added the following lines to the manuscript (Lines 741 to 761):

Moreover, the maximum value of Δ on the compression side is reached at a lower strain level for TR0 compared to TR45 and TR90 samples. This trend is consistent with the stress ratio variations shown in Figures 3 (a), (b), and (c), where the maximum stress ratio for TR0 samples is attained at a lower ε_q compared to TR45 and TR90 samples. Comparing Figure 3(a) with Figures 13(a-c) and Figure 14(a), it is evident that the changes in magnitudes of the stress ratios correspond closely to those of the diagonal components and invariant of the fabric tensor. For instance, F_x, F_y, and F_z vary alternatively between a maximum and minimum when the loading direction is reversed. The same trend is observed for the stress ratio in Figure 3(a). When $\eta > 0$, the value of fabric components continuously increases, while they decrease gradually when $\eta < 0$. In the context of three-dimensional DEM modeling of assemblies subjected to triaxial compression, [4] analytically derived the correlation between stress and fabric tensor invariants. [24] also emphasized a distinct relationship between the anisotropic distribution of contact normals and the mobilized stress ratio in real sands.

REVIEWER C – 24. Is the CN = 4 limit applicable to all granular materials, or would it depend on gradation and particle shape?

Response:
Thank you very much for this constructive comment. We do acknowledge that the jamming transition depends on pressure, friction as well as particle shape parameters including asphericity and aspect ratio. Regardless of particle characteristics and from a physical perspective, the threshold value of 4 holds significance for both mechanical stability and degrees of freedom. In three-dimensional space, at least four non-coplanar connections are necessary to achieve static mechanical stability. This aligns with Maxwell's criterion for rigidity—when a particle has fewer than four connections, it retains excessive degrees of freedom, preventing it from maintaining a stable position relative to its neighbors. Moreover, as the coordination number exceeds 4, translational motion becomes increasingly restricted, rotational degrees of freedom are significantly constrained, and the energy required for structural rearrangement rises substantially. In the literature, many studies have used different particle assemblies with various shapes, including spheres and elongated particles with different gradations. These studies have reported specific coordination number values that indicate the transition from solid-like to fluid-like behavior. For example, considering only the non-floaters and force-bearing contacts, [36] suggested a coordination number of 4 as the assembly with spherical particles reaches the onset of initial liquefaction. Other studies mainly consider particles with two or more contacts in the definition of mechanical coordination number (MCN) and documented a value of MCN= 3 (e.g., [8])

or MCN= 3.2 (e.g., [20]) at the liquefied state of a granular assembly. We also added the mentioned description in reply to Comment 5.

Review Round 2

Author response (general)

The authors wish to thank the reviewers and editor for their time and efforts in reviewing our manuscript. We hope the modified manuscript is suitable for publication in the Journal of Open Geomechanics. In the following, detailed answers to the reviewer's comments are provided. Changes addressing the reviewers' remarks are highlighted in yellow in the 'Tracked Changes' version of the manuscript.

Reviewer A (Mehdi Pouragha)

The authors have responded to the comments raised in the first round of reviews in an exemplary manner, which is greatly appreciated. The revisions made to the manuscript address many of the concerns previously highlighted.

However, the issue concerning the damping ratio remains unresolved. In their response, the authors refer to the coefficient of restitution (CoR) and suggest a link to the Cundall damping ratio. It is unclear, however, how the reported range of CoR is quantitatively translated into a corresponding range of numerical damping values. Reference [29] by Kuhn et al. is cited in support of the chosen damping ratio, yet, to my knowledge, this study does not report a damping ratio. I invite the authors to clarify how this particular reference substantiates their selection.

The authors also refer to the work by Zhou et al. [40], in which it is shown that the damping ratio has a negligible effect on the angle of repose. However, this response does not address my original concern, which relates to the potential rate-dependence of the results arising from the use of a high damping ratio. For example, preliminary findings such as those presented in DOI: 10.1061/(ASCE)EM.1943-7889.0000889 suggest a non-negligible effect of damping ratio on microstructure. I suspect this effect is more pronounced for the cyclic tests considered in the current study.

The authors are therefore encouraged either to provide clear justification or evidence that the selected damping ratio has been appropriately calibrated to produce realistic results, or to acknowledge that this aspect has not been fully explored and explicitly state that it remains an open question. As currently written, the manuscript implies that the chosen damping ratio is appropriate, without sufficient supporting evidence, which could be misleading to readers.

Reviewer C (Alejandro Martinez)

The authors have addressed all of my comments. Therefore, my recommendation is to accept the paper for publication.

Author response

REVIEWER A

We deeply appreciate the reviewer's efforts to thoroughly review the paper and provide his/her insightful comments, which significantly contribute to the improvement of our manuscript. We acknowledge that the effect of the damping ratio has not been systematically investigated in this study. In light of this, we have revised the manuscript to explicitly state that the selected damping ratio was not calibrated through a dedicated sensitivity analysis and that its influence remains an open question that merits further investigation in future work. The following lines have been added to the manuscript:

A damping ratio of 0.7 is assumed. It is important to note that the specific influence of the damping ratio is beyond the scope of this study and remains an open question for future research.

REVIEWER C

We deeply appreciate the reviewer's efforts to thoroughly review the paper and provide his/her insightful comments, which significantly contribute to the improvement of our manuscript.

References

[1] Ajam Norouzi, M. and Seyedi Hosseininia, E. (2024). Effect of initial fabric anisotropy on cyclic liquefaction behavior of granular soils using discrete element method. *Granular Matter*, 26(2):25.

[2] Basson, M. S., Martinez, A., and DeJong, J. T. (2024). Dem simulations of the liquefaction resistance and post-liquefaction strain accumulation of coarse-grained soils with varying gradations. *Computers and Geotechnics*, 174:106649.

[3] Flores-Johnson, E., Wang, S., Maggi, F., El Zein, A., Gan, Y., Nguyen, G., and Shen, L. (2016). Discrete element simulation of dynamic behaviour of partially saturated sand. *International Journal of Mechanics and Materials in Design*, 12:495–507.

[4] Gao, Z., Zhao, J., Li, X.-S., and Dafalias, Y. F. (2014). A critical state sand plasticity model accounting for fabric evolution. *International journal for numerical and analytical methods in geomechanics*, 38(4):370–390.

[5] Gong, G. (2008). *DEM [Discrete Element Method] simulations of drained and undrained behaviour*. PhD thesis, University of Birmingham.

[6] Gong, G. and Zha, X. (2013). Dem simulation of undrained behaviour with preshearing history for saturated granular media. *Modelling and Simulation in Materials Science and Engineering*, 21(2):025001.

[7] Gu, X., Huang, M., and Qian, J. (2014). Dem investigation on the evolution of microstructure in granular soils under shearing. *Granular Matter*, 16(1):91–106.

[8] Gu, X., Zhang, J., and Huang, X. (2020). Dem analysis of monotonic and cyclic behaviors of sand based on critical state soil mechanics framework. *Computers and Geotechnics*, 128:103787.

[9] Hakuno, M. and Tarumi, Y. (1988). Sand liquefaction analysis by granular assembly simulation. In *Proceedings of ninth world conference on earthquake engineering*, volume 8, pages 231–236.

[10] Holtz, R. D., Kovacs, W. D., and Sheahan, T. C. (1981). *An introduction to geotechnical engineering*, volume 733. Prentice-Hall Englewood Cliffs.

[11] Iai, S., Tobita, T., and Ozutsumi, O. (2013). Induced fabric under cyclic and rotational loads in a strain space multiple mechanism model for granular materials. *International Journal for Numerical and Analytical Methods in Geomechanics*, 37(2):150–180.

[12] Irani, N., Salimi, M., Golestaneh, P., Tafili, M., Wichtmann, T., and Lederer, J. (2024). Deep learning-based analysis of true triaxial dem simulations: Role of fabric and particle aspect ratio. *Computers and Geotechnics*, 173:106529.

[13] Jiang, M., Zhang, A., and Li, T. (2019). Distinct element analysis of the microstructure evolution in granular soils under cyclic loading. *Granular Matter*, 21:1–16.

[14] Kantak, A. A. and Davis, R. H. (2006). Elastohydrodynamic theory for wet oblique collisions. *Powder technology*, 168(1):42–52.

[15] Kuhn, M. R. (2006). Oval and ovalplot: Programs for analyzing dense particle assemblies with the discrete element method. *Department of Civil Engineering, University of Portland, Portland, OR, USA*.

[16] Kuhn, M. R., Renken, H. E., Mixsell, A. D., and Kramer, S. L. (2014). Investigation of cyclic liquefaction with discrete element simulations. *Journal of Geotechnical and Geoenvironmental Engineering*, 140(12):04014075.

[17] Liu, A. J. and Nagel, S. R. (2010). The jamming transition and the marginally jammed solid. *Annu. Rev. Condens. Matter Phys.*, 1(1):347–369.

[18] Liu, G., Rong, G., Peng, J., and Zhou, C. (2015). Numerical simulation on undrained triaxial behavior of saturated soil by a fluid coupled-dem model. *Engineering Geology*, 193:256–266.

[19] Lopera Perez, J., Kwok, C., O'Sullivan, C., Huang, X., and Hanley, K. (2016). Exploring the micro-mechanics of triaxial instability in granular materials. *Géotechnique*, 66(9):725–740.

[20] Martin, E. L., Thornton, C., and Utili, S. (2020). Micromechanical investigation of liquefaction of granular media by cyclic 3d dem tests. *Géotechnique*, 70(10):906–915.

[21] Mitchell, J. K., Soga, K., et al. (2005). *Fundamentals of soil behavior*, volume 3. John Wiley & Sons New York.

[22] Mo, W., Wang, R., Zhang, J.-M., and Dafalias, Y. F. (2024). Quantification of fabric evolution in granular material under cyclic loading. *International Journal for Numerical and Analytical Methods in Geomechanics*, 48(3):701–726.

[23] Ni, X., Ma, J., and Zhang, F. (2024). Mechanism of the variation in axial strain of sand subjected to undrained cyclic triaxial loading explained by dem with non-spherical particles. *Computers and Geotechnics*, 165:105846.

[24] Oda, M. (1972). The mechanism of fabric changes during compressional deformation of sand. *Soils and foundations*, 12(2):1–18.

[25] O'Hern, C. S., Langer, S. A., Liu, A. J., and Nagel, S. R. (2002). Random packings of frictionless particles. *Physical Review Letters*, 88(7):075507.

[26] Okada, Y. and Ochiai, H. (2007). Coupling pore-water pressure with distinct element method and steady state strengths in numerical triaxial compression tests under undrained conditions. *Landslides*, 4(4):357–369.

[27] Pires-Sturm, A. P. and DeJong, J. T. (2022). Influence of particle size and gradation on liquefaction potential and dynamic response. *Journal of Geotechnical and Geoenvironmental Engineering*, 148(6):04022045.

[28] Radjai, F. and Dubois, F. (2011). *Discrete-element modeling of granular materials*. Wiley-Iste.

[29] Salimi, M. and Lashkari, A. (2020). Undrained true triaxial response of initially anisotropic particulate assemblies using cfm-dem. *Computers and Geotechnics*, 124:103509.

[30] Salimi, M., Lashkari, A., and Tafili, M. (2024). Dem investigation on flow instability of particulate assemblies under coupling between volumetric and axial strains. *Acta Geotechnica*, pages 1–26.

[31] Salimi, M., Tafili, M., Irani, N., and Wichtmann, T. (2023a). Micro-mechanical response of transversely isotropic samples under cyclic loading. In *10th European Conference on Numerical Methods in Geotechnical Engineering (NUMGE2023)*, pages 1–6.

[32] Salimi, M., Tafili, M., Irani, N., and Wichtmann, T. (2023b). Micro-mechanical response of transversely isotropic samples under cyclic loading. *10th European Conference on Numerical Methods in Geotechnical Engineering*.

[33] van Hecke, M. (2009). Jamming of soft particles: geometry, mechanics, scaling and isostaticity. *Journal of Physics: Condensed Matter*, 22(3):033101.

[34] Wei, J., Huang, D., and Wang, G. (2020). Fabric evolution of granular soils under multidirectional cyclic loading. *Acta Geotechnica*, 15:2529–2543.

[35] Yang, M. and Taiebat, M. (2024). Exploring the role of fabric anisotropy in cyclic liquefaction resistance under non-hydrostatic consolidation: Insights from dem analysis. In *E3S Web of Conferences*, volume 544, page 10011. EDP Sciences.

[36] Yang, M., Taiebat, M., Mutabaruka, P., and Radjai, F. (2021). Evolution of granular materials under isochoric cyclic simple shearing. *Physical Review E*, 103(3):032904.

[37] Yuan, Y., VanderWerf, K., Shattuck, M. D., and O'Hern, C. S. (2019). Jammed packings of 3d superellipsoids with tunable packing fraction, coordination number, and ordering. *Soft matter*, 15(47):9751–9761.

[38] Zhang, A., Jiang, M., and Wang, D. (2023). Effect of fabric anisotropy on the cyclic liquefaction of sands: Insight from dem simulations. *Computers and Geotechnics*, 155:105188.

[39] Zhao, J., Zhu, Z., Zhang, D., Wang, H., and Li, X. (2024). Assessment of fabric characteristics with the development of sand liquefaction in cyclic triaxial tests: A dem study. *Soil Dynamics and Earthquake Engineering*, 176:108343.

[40] Zhou, Y., Xu, B. H., Yu, A.-B., and Zulli, P. (2002). An experimental and numerical study of the angle of repose of coarse spheres. *Powder technology*, 125(1):45–54.

[41] Zhu, M., Gong, G., Xia, J., Liu, L., and Wilkinson, S. (2021). Effects of deviator strain histories on liquefaction of loose sand using dem. *Computers and Geotechnics*, 136:104213.